INTERNATIONAL JOURNAL OF HEAT AND TECHNOLOGY
Vol.33, No.1, 2015

ANALYSIS OF CONDUCTION-RADIATION HEAT TRANSFER WITH VARIABLE THERMAL CONDUCTIVITY AND VARIABLE REFRACTIVE INDEX: APPLICATION OF THE LATTICE BOLTZMANN METHOD

Ahmed Mahmoudi [1] and Imen Mejri [1]

[1] Unité de Recherche Matériaux, Energie et Energies Renouvelables (MEER), Faculté des Sciences de Gafsa, B.P.19, Zarroug, Gafsa, 2112, Tunisie

ABSTRACT

The effect of variable thermal conductivity and variable refractive index on transient conduction and radiation heat transfer in a planar medium is investigated. Thermal conductivity of the medium is assumed to vary linearly with temperature, while the other thermo-physical properties are assumed constant. The radiative transfer equation and the nonlinear energy equation are solved using lattice Boltzmann method (LBM). The effects of various parameters are studied. The LBM results are compared with those available in literature and a good agreement is found.

Keywords: Lattice Boltzmann method, Conduction, Radiation, Planar medium.

1. INTRODUCTION

Combined conduction-radiation heat transfer has numerous engineering applications such as heat transfer through semitransparent and porous materials, multilayered insulations, burning of coal in furnaces, fluidized beds, nuclear engineering, and so on. The cases of constant thermal conductivity and unity refractive index in combined conduction–radiation heat transfer problems have been studied in detail by many investigators [1-5]. Because of the mathematical complexities, a limited literature is available that individually deal with the effects of variable thermal conductivity [6] and constant and/or variable refractive index [7]. The case of variable thermal conductivity and variable refractive index finds application in the thermal analysis of graded index medium [8]. The present work is, therefore, aimed at the analysis of conduction and radiation heat transfer in a participating medium, by lattice Boltzmann method. The effect of variable thermal conductivity and constant and/or variable refractive index are considered. In recent years, use of the lattice Boltzmann method (LBM) as a potential computational fluid dynamics (CFD) tool for the solution of a large class of problems in science and engineering has gained a momentum. Chaabane et al. [9] used the lattice boltzmann method to solve the energy equation in two dimensional enclosure of a problem involving a variety of boundary conditions, they found that the LBM results agree very well with the finite volume results. Mejri et al. [10] studied 1-D conduction-radiation problem by lattice Boltzmann method. LBM is used to solve the energy equation and the radiative transfer equation. The found results are compared with those available in the literature and a very good agreement was found. Lorenzini et al. [11] optimized the dimensionless excess of temperature of an open T-shaped cavity cooled by a steady stream of convection that intrudes into a solid conducting wall subject to an area fraction. Lorenzini et al. [12] Lorenzini et al. optimized the shape of cavities that intrude into a cylindrical solid body. The objective is to minimize the global thermal resistance between the solid body and the cavities. The results indicate that the optimal distribution of the hot spots is affected not only by the complexity of the configuration (larger N) but also by the area of cavities fraction. Mahmoudi et al. [13] studied MHD natural convection in a nanofluid-filled open cavity with non uniform boundary condition in the presence of uniform heat generation/absorption. The found results show that the heat transfer rate decreases with the rise of the Hartmann number and increases with the augmentation of the Rayleigh number. Mahmoudi et al. [14] studied the effect of the magnetic field intensity and direction on natural convection in a square enclosure filled with nanofluid. The found results show that the heat transfer and fluid flow depends strongly upon the direction of magnetic field. Mejri et al. [15] studied magnetic field effect on natural convection in a nanofluid filled enclosure with non-uniform heating on both side walls. The authors used lattice Boltzmann method to solve the coupled equations of flow and temperature fields. The found results show that the heat transfer rate increases with the increase of the Rayleigh number but it decreases with the increase of the Hartmann number.

In this paper, the 1-D conduction-radiation problem with variable thermal conductivity and variable refractive index is solved by the lattice Boltzmann method. The effects of various parameters such as the scattering albedo, the conduction–radiation parameter, the wall emissivity and the thermal conductivity parameter are studied. In order to check on the accuracy of the numerical technique employed for the solution of the considered problem, the present numerical code was validated with the published study.

2. MATHEMATICAL FORMULATION

Consider a 1-D planar conducting–radiating medium of length L, with variable thermal conductivity *k*. Other thermo-physical properties such as density ρ, specific heat c_p, and optical properties such as extinction coefficient β and scattering albedo ω are assumed constant. The system is initially at temperature T_E and for time t > 0, its west boundary is raised to temperature T_W. The variation of thermal conductivity with temperature is taken as:

$$k = k_0 + \delta'(T - T_w) \tag{1}$$

Where k_0 is the reference thermal conductivity and δ' is the coefficient of thermal conductivity variation. The refractive index *n* of the medium assumes either a constant value ($n \geq 1$) or varies linearly with distance $n(x) = n_W + (n_W - n_E)x/L$, where n_W and n_E are the refractive indices on the west and the east faces of the medium, respectively. For the problem under consideration, the energy equation is given by:

$$\rho c_P \frac{\partial T}{\partial t} = -\frac{\partial}{\partial x}(-k\frac{\partial T}{\partial x}) - \frac{\partial q_R}{\partial x} \tag{2}$$

Where q_R is the radiative heat flux and $\frac{\partial q_R}{\partial x}$ for a medium with a variable refractive index is given by:

$$\frac{\partial q_R}{\partial x} = \beta(1-\omega)(4n^2\pi\frac{\sigma T^4}{\pi} - G) \tag{3}$$

G is the incident radiation. To solve for G at any location *x*, information about the intensity *I* distribution is required which for any direction $\vec{s}$ is obtained from the following radiative transfer equation:

$$\frac{1}{c}\frac{\partial I(\vec{x},\vec{s},t)}{\partial t} + \frac{\partial I(\vec{x},\vec{s},t)}{\partial s} = -\beta I(\vec{x},\vec{s},t) + \beta(1-\omega)I_b(\vec{x},t) + \frac{\beta\omega}{4\pi}\int_{\Omega'=4\pi} I(\vec{x},\vec{s},t)p(\vec{s}'\to\vec{s})d\Omega' \tag{4}$$

Where *c* is the speed of light in the medium, $I_b = n^2\sigma T^4/\pi$ is the Planck's black body intensity, $d\Omega$ is the solid angle and $p(\vec{s}'\to\vec{s})$ is the anisotropic scattering phase function. For a given direction $\vec{s}$, if the upstream point lies on the boundary, then its values have to be computed from the radiative boundary condition. Eq. (4) can be recast as:

$$\frac{1}{c}\frac{\partial I(\vec{x},\vec{s},t)}{\partial t} + \vec{s}.\nabla I(\vec{x},\vec{s},t) = -\beta I(\vec{x},\vec{s},t) + \beta S(\vec{x},\vec{s},t) \tag{5}$$

Where S is the radiative source term given as:

$$S(\vec{x},\vec{s},t) = (1-\omega)I_b(\vec{x},t) + \frac{\omega}{4\pi}\int_{\Omega'=4\pi} I(\vec{x},\vec{s},t)p(\vec{s}'\to\vec{s})d\Omega' \tag{6}$$

For a linear anisotropic phase function $p = 1 + a\cos\gamma\cos\gamma'$, where a is the anisotropy factor $(-1 < a < 1)$, Eq. (6) can be written as:

$$S(\vec{x},\vec{s},t) = (1-\omega)I_b(\vec{x},t) + \frac{\omega}{4\pi}\int_{\Omega'=4\pi} I(\vec{x},\vec{s},t)(1 + a\cos\gamma\cos\gamma')d\Omega' \tag{7}$$

$$S(\vec{x},\vec{s},t) = (1-\omega)I_b(\vec{x},t) + \frac{\omega}{4\pi}\left[G(\vec{x},t) + a\cos\gamma q_R(\vec{x},t)\right] \tag{8}$$

γ is the polar angle.

$$G = 2\pi\int_{\gamma=0}^{\pi} I(\gamma)\sin(\gamma)d\gamma \tag{9}$$

$$q_R = 2\pi\int_{\gamma=0}^{\pi} I(\gamma)\cos(\gamma)\sin(\gamma)d\gamma \tag{10}$$

For a diffuse-gray boundary with temperature $T_{E/W}$ and emissivity $\varepsilon_{E/W}$, the boundary intensity is given by:

$$I(\vec{x}_E,\vec{s}) = \varepsilon_E I_b(\vec{x}_E) + \frac{(1-\varepsilon_E)}{\pi}\int_{\Omega'=2\pi}\left[|I(\vec{x}_E,\vec{s})|\vec{n}.\vec{s}\right]_{\vec{n}.\vec{s}>0}d\Omega' \tag{11}$$

$$I(\vec{x}_W,\vec{s}) = \varepsilon_W I_b(\vec{x}_W) + \frac{(1-\varepsilon_W)}{\pi}\int_{\Omega'=2\pi}\left[|I(\vec{x}_W,\vec{s})|\vec{n}.\vec{s}\right]_{\vec{n}.\vec{s}<0}d\Omega' \tag{12}$$

For solving the considered problem, the following dimensionless numbers are defined:

$$N = \frac{k_0\beta}{4\sigma T_w^3}\ ,\ \xi = \alpha\beta^2 t\ ,\ \delta = \frac{\delta' T_w N}{k_0} \tag{13}$$

N is the conduction–radiation parameter, ξ is the dimensionless time and δ is the variable thermal conductivity parameter.

2.1 Energy equation by LBM

For a one-dimensional planar geometry, in the LBM with a D1Q2 lattice, the discrete Boltzmann equation with Bhatanagar- Gross-Krook (BGK) approximation is given by [8]:

$$\frac{\partial f_i(\vec{x},t)}{\partial t} + \vec{e}_i.\nabla f_i(\vec{x},t) = -\frac{1}{\tau}\left[f_i(\vec{x},t) - f^{eq}_i(\vec{x},t)\right]\quad i = 1 \text{ and } 2 \tag{14}$$

Where f_i is the particle distribution function denoting the number of particles at the lattice node $\vec{x}$ and time *t* moving in direction *i* with velocity $\vec{e}_i$ along the lattice $\Delta x = e_i\Delta t$ connecting the neighbors, τ is the relaxation time, and f^{eq}_i is the equilibrium distribution function. The relaxation time τ for the D1Q2 lattice is computed from:

$$\tau = \frac{k}{\rho c_p |\vec{e}_i|^2} + \frac{\Delta t}{2} \qquad (15)$$

For this lattice, the two velocities e_1 and e_2, and their corresponding weights w_1 and w_2, are given by:

$$e_1 = \frac{\Delta x}{\Delta t} \qquad e_2 = -\frac{\Delta x}{\Delta t} \qquad (16)$$

$$w_1 = w_2 = \frac{1}{2} \qquad (17)$$

After discretization, Eq. (14) is written as:

$$f_i(\vec{x}+\vec{e}_i\Delta t,\ t+\Delta t) = f_i(\vec{x},t) - \frac{1}{\tau}\left[f_i(\vec{x},t) - f^{eq}{}_i(\vec{x},t)\right] \qquad (18)$$

The temperature is obtained after summing f_i overall direction:

$$T(\vec{x},t) = \sum_{i=1,2} f_i(\vec{x},t) \qquad (19)$$

To process Eq. (18), an equilibrium distribution function is required, which for a conduction-radiation problem is given by:

$$f^{eq}{}_i(\vec{x},t) = w_i T(\vec{x},t) \qquad (20)$$

To account for the volumetric radiation, the energy equation in the LBM formulation, Eq. (18) is modified to:

$$f_i(\vec{x}+\vec{e}_i\Delta t,\ t+\Delta t) = f_i(\vec{x},t) - \frac{1}{\tau}\left[f_i(\vec{x},t) - f^{eq}{}_i(\vec{x},t)\right] - \frac{\Delta t\ w_i}{\rho c_P}\frac{\partial q_R}{\partial x} \qquad (21)$$

2.2 Radiative information by LMB

Multiplying Eq.(5) throughout by the speed of light *c*, the radiative transfer equation along any lattice link designated by the index *i* can be written as:

$$\frac{DI_i}{Dt}(\vec{x},\vec{s},t) = \frac{\partial I_i}{\partial t} + \vec{c}.\nabla I_i = -c\beta(I_i - S_i) \qquad i=1,...,M \qquad (22)$$

Let $\vec{e}_i$ be the velocity of propagation along the *i*th lattice link of the D1QM lattice structure. If the velocity of light $\vec{c}$ is fictitiously made equal to the velocity of particle propagation in the LBM, $\vec{c} = \vec{e}$ a convenient tool would be obtained to solve the radiative transfer equation using the LBM approach

$$\frac{\partial I_i}{\partial t} + \vec{e}_i.\nabla I_i = e_i\beta(S_i - I_i) \qquad i=1,...,M \qquad (23)$$

Discretizing Eq. (23), we obtain:

$$I_i(\vec{x}+\vec{e}_i\Delta t,\ t+\Delta t) = I_i(\vec{x},t) + \Delta t e_i\beta(S_i - I_i) \quad i=1,...,M \qquad (24)$$

Clearly in Eq. (24), the term on the right hand side can be seen as the collision term in the LBM, where I_i is the intensity particle distribution function. Using the standard LBM terminology, Eq. (24) can be written as:

$$I_i(\vec{x}+\vec{e}_i\Delta t,\ t+\Delta t) = I_i(\vec{x},t) + \frac{\Delta t}{\tau_R}\left[I_i^{eq}(\vec{x},t) - I_i(\vec{x},t)\right] \qquad (25)$$

Where τ_R is the relaxation time for the collision process and I_i^{eq} is the equilibrium particle distribution function.

$$\tau_R = \frac{1}{e_i\beta} \quad \text{and} \quad I_i^{eq} = S_i \qquad (26)$$

The irradiation *G* and the heat flux q_R due to diffuse radiation, are computed from the following:

$$G = 4\pi \sum_{i=1,M} I_i \sin\gamma_i \sin(\frac{\Delta\gamma_i}{2}) \qquad (27)$$

$$q_R = 2\pi \sum_{i=1,M} I_i \sin\gamma_i \cos\gamma_i \sin(\Delta\gamma_i) \qquad (28)$$

3. RESULTS AND DISCUSSION

In this paper, the energy equation of a 1-D transient conduction- radiation problem with variable thermal conductivity *k*, is solved with LBM. Initially the medium is at temperature T_E. For $t > 0$, the west boundary temperature is maintained at $T_W = 2T_E$. The medium is absorbing, emitting and isotropically scattering. The non dimensional time step $\Delta\xi = 10^{-4}$ was considered and steady state condition was assumed to have been achieved when the maximum variation in temperature at any location between two consecutive time levels did not exceed 10^{-5}. First the effect of the grid size to the non-dimensional temperature results (T/T_w) is studied by comparing the steady state (SS) results at three locations in the medium for several grid sizes for n = 1, δ = 0, a = 0, β=1.0, N=0.1, T_E=0.0, T_w=1.0, ω=0.5 and $\varepsilon_w = \varepsilon_E$ = 1.0. The results are listed in **table.1** and show that the non-dimensional temperature is practically independent of the grid size. In **table.2**, for ξ = 0.05, n = 1, δ = 0, a = 0, β=1.0, N=0.1, T_E=0.0, T_w=1.0, ω=0.5, ε_w =1.0 and ε_E = 1.0 or 0.0, the non-dimensional temperature results (T/T_w) are compared with those reported in the literature [1-2] at three locations in the medium, It is observed that the LBM results are in good agreements with the published results.

Fig.1a-c shows the effect of the conduction-radiation parameter by comparing the LBM results (T/T_w) with those published at several times ξ, for n = 1, δ = 0, a = 0, β=1.0, ω = 0.0 and N = 0.01, 0.1 and 1.0. The LBM results are in good agreements with the published results.

Fig.2a-c shows for several times the effect of the scattering albedo ω=0.0, 0.5 and 0.9 for n = 1, δ = 0, a = 0, β =1.0 and N=0.01 by comparing the LBM results (T/T_w) with those published. Excellent agreement is also found.

Table 1. Effect of grid size on non-dimensional temperature steady state

		x/L = 0.25	x/L = 0.50	x/L = 0.75
N_x=20	M=4	0.8265	0.6076	0.3339
	M=8	0.8356	0.6204	0.3438
	M=16	0.8389	0.6254	0.3479
	M=32	0.8400	0.6270	0.3492
M=32	N_x=20	0.8400	0.6270	0.3492
	N_x=30	0.8438	0.6210	0.3365
	N_x=40	0.8269	0.6181	0.3441
	N_x=60	0.8227	0.6152	0.3425

Table 2. Comparison of transient temperature

		x/L = 0.25	**x/L = 0.5**	**x/L = 0.75**
$\varepsilon_W = 1.0$	[1]	0.4888	0.1778	0.0591
	[2]	0.4889	0.1773	0.0588
$\varepsilon_E = 1.0$	LBM	0.4893	0.1787	0.05724
$\varepsilon_W = 1.0$	[1]	0.5030	0.2005	0.0833
	[2]	0.5031	0.2001	0.0830
$\varepsilon_E = 0.0$	LBM	0.5037	0.1993	0.0841

a
b
c

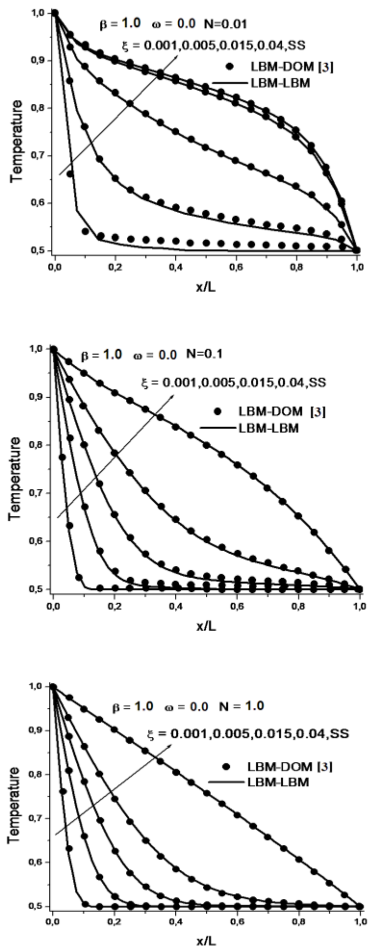

Figure 1. Comparison of the non dimensional temperature (T/T_w) at different instants ξ for (a) N = 0.01, (b) 0.1 and (c) 1.0

a
b
c

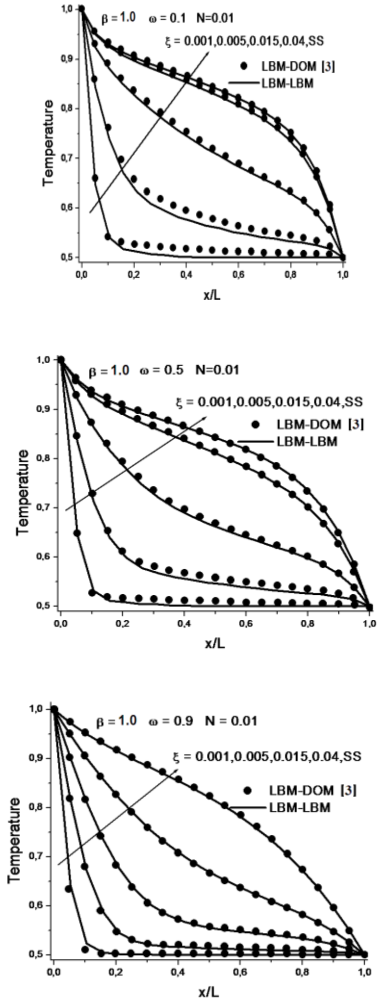

Figure 2. Comparison of the non dimensional temperature (T/T_w) at different ξ for (a) ω=0.1, (b) 0.5 and (c) 0.9

Fig.3a-c show the effect of the emissivity ε_W = 0.1, 0.5 and 0.9 by comparing the LBM results (T/T_w) with those published for n = 1, δ = 0, a = 0, β = 1.0, ω=0.0, N=0.01 and ε_E=1.0. It is shown that the LBM results are in good agreements with the published results.

Fig.4 shows the effect of the extinction coefficient by comparing the steady-state (SS) results obtained by the LBM and the published results, for n = 1, δ = 0, a = 0, ω=0.0 and N = 0.1. These comparisons are shown for β = 0.1, 1.0 and 2.0. Excellent agreement is also found.

Fig.5a-b shows the effect of the variable thermal conductivity parameter for different extinction coefficients (β = 0.1 and 1.0) by comparing the steady-state results obtained by the LBM and the published results, for n = 1, a = 0, ω=0.5, N = 0.5, ε_w = 1.0 and ε_E = 0.5.The LBM results are in good agreement with those published.

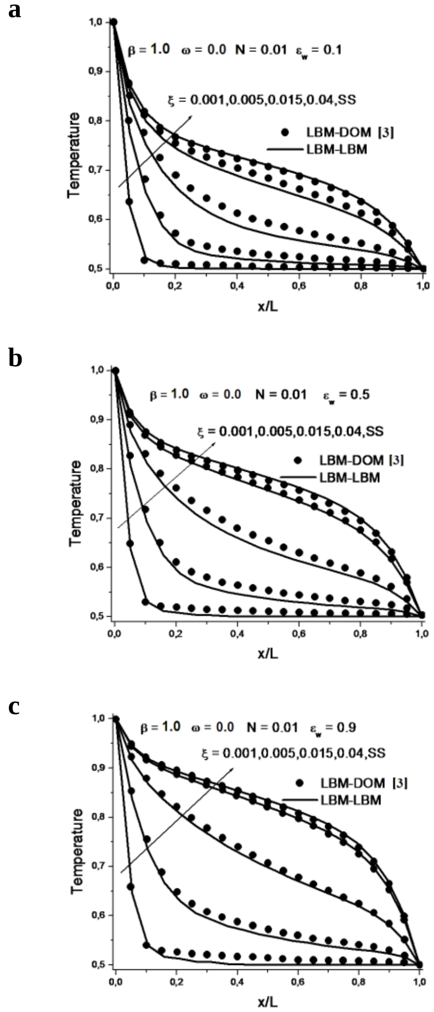

Figure 3. Comparison of the non dimensional temperature (T/T_w) at different ξ for (a) $\varepsilon_W = 0.1$, (b) 0.5 and (c) 0.9

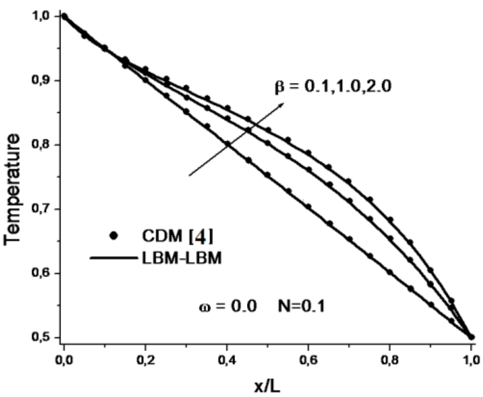

Figure 4. Comparison of the non dimensional temperature (T/T_w) for different β

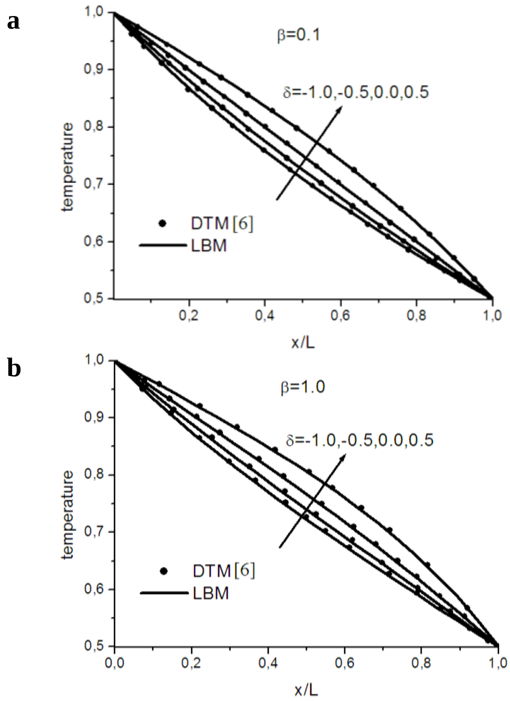

Figure 5. Comparison of the non dimensional temperature (T/T_w) for different δ for (a) β = 0.1 and (b) β = 1.0

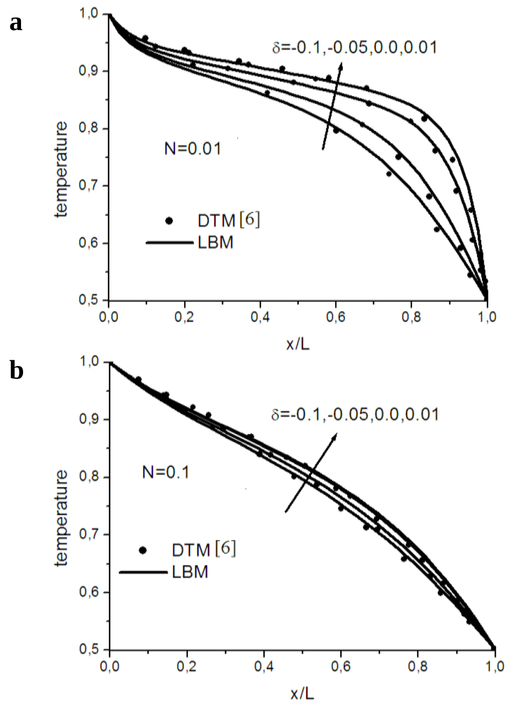

Figure 6. Comparison of the non dimensional temperature (T/T_w) for different δ for (a) N = 0.01 and (b) N = 0.1

Fig.6a-b shows the effect of the variable thermal conductivity parameter for different conduction– radiation parameters (N = 0.01 and 0.1) by comparing the steady-state results obtained by the LBM and the published results, for $n = 1$, $a = 0$, ω=0.0, β = 1.0, $\varepsilon_w = 1.0$ and $\varepsilon_E = 0.5$. The LBM results are in good agreement with those published.

Fig.7a-c shows the effect of the variable thermal conductivity parameter for different scattering albedo (ω = 0.0, 0.5 and 0.1) by comparing the steady-state results obtained by the LBM and the published results, for $a = 0$, N=0.5, β = 1.0,

ε_w = 1.0 and ε_E = 0.5. The LBM results are in good agreement with those published.

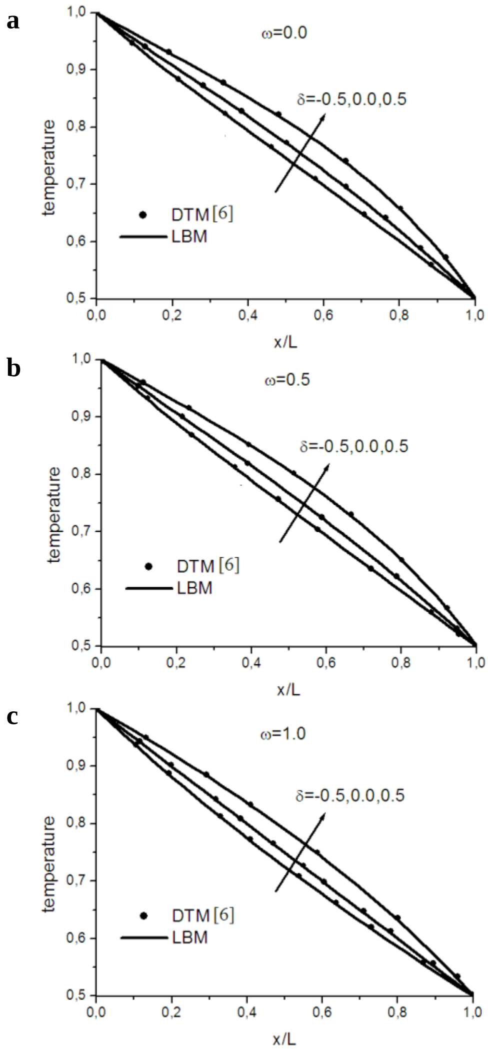

Figure 7. Comparison of the non dimensional temperature (T/T_w) for different δ for (a) ω = 0.0, (b) 0.5 and (c) 0.9

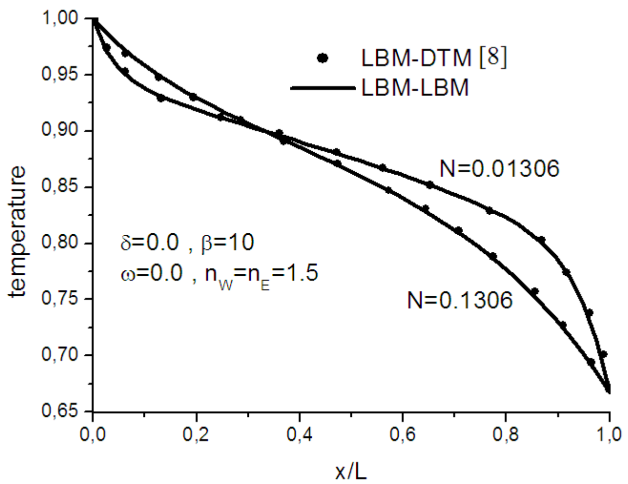

Figure 8. Comparison of the non dimensional temperature (T/T_w) for different N

Fig.8 shows the effect of the conduction– radiation parameter for n_E =n_W=1.5 by comparing the steady-state results obtained by the LBM and the published results, for a = 0, ω=0.0, β = 10.0, $\varepsilon_w = \varepsilon_E$ = 1.0, δ=0.0 and T_W =3T_E. The LBM results are in good agreement with those published.

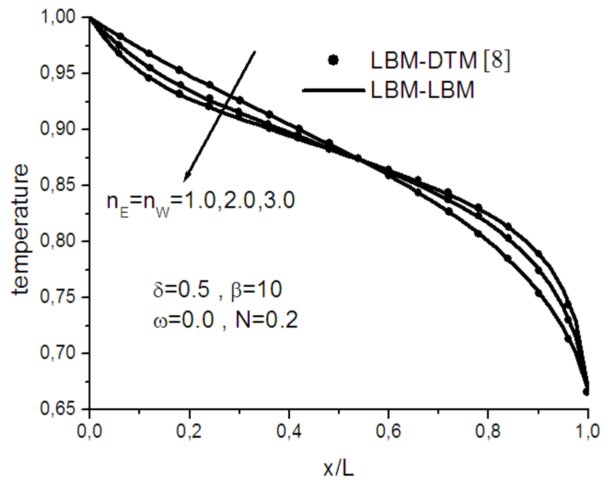

Figure 9. Comparison of the non dimensional temperature (T/T_w) for different refractive index

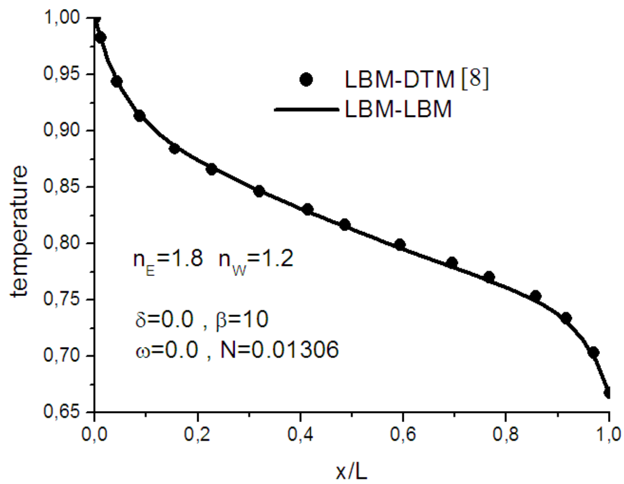

Figure 10. Comparison of the non dimensional temperature (T/T_w) for variable refractive index

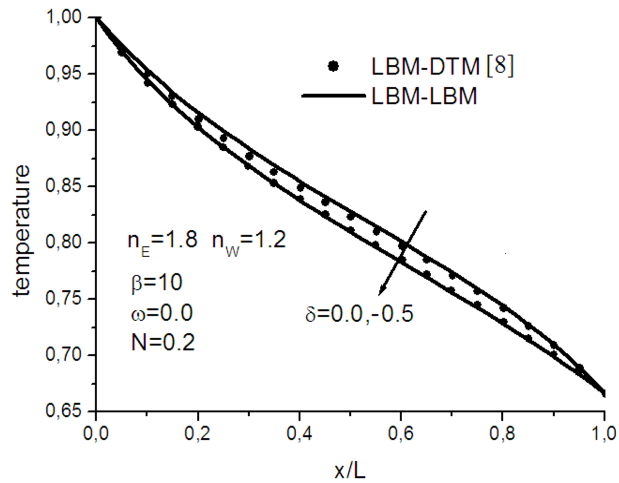

Figure 11. Comparison of the non dimensional temperature (T/T_w) for variable refractive index

Fig.9 shows the effect of the refractive index by comparing the steady-state results obtained by the LBM and the published results, for a = 0, ω=0.0, β = 10.0, $\varepsilon_w = \varepsilon_E$ = 1.0,

δ=0.5, N=0.2 and T_W =3T_E. The LBM results are in good agreement with those published.

Fig.10 and **11** show the effect of the variable refractive index for different conduction– radiation parameters and different variable thermal conductivity parameters by comparing the steady-state results obtained by the LBM and the published results, for *a* = 0, ω=0.0, β = 10.0, $\varepsilon_w = \varepsilon_E = 0.0$ and T_W =3T_E. The LBM results are in good agreement with those published.

4. CONCLUSIONS

The LBM is used to analyze combined conduction–radiation heat transfer in a planar absorbing, emitting and scattering medium with variable thermal conductivity and variable refractive index. The radiative information and the energy equation are solved using the LBM. The results of the LBM-LBM formulation are compared with those available in the literature. A very good agreement was found.

REFERENCES

1. S.C. Mishra, A. Lankadasu, Analysis of Transient Conduction and Radiation Heat Transfer Using the Lattice Boltzmann Method and the Discrete Transfer Method, *Numerical Heat Transfer, Part A*, vol.47, pp. 935–954, 2005.
2. R. Raj , A. Prasad , P.R. Parida, S.C. Mishra, Analysis of Solidification of a Semi transparent Planar Layer Using the Lattice Boltzmann Method and the Discrete Transfer Method, *Numerical Heat Transfer, Part A*, vol.49, pp. 279–299, 2006.
3. B. Mondal, S.C. Mishra, Application of the lattice boltzmann method and the discrete ordinates method for solving transient conduction and radiation heat transfer problems, *Numerical Heat Transfer, Part A*, vol.52, pp. 757–775, 2007.
4. S.C. Mishra, P. Talukdar, D. Trimis, F. Durst, Computational efficiency improvements of the radiative transfer problems with or without conduction-a comparison of the collapsed dimension method and the discrete transfer method, *Int J of Heat and Mass Transfer*, vol. 46, 3083–3095, 2003.
5. S.C. Mishra, R.R Vernekar, Analysis of transport of collimated radiation in a participating media using the lattice Boltzmann method, *Journal of Quantitative Spectroscopy & Radiative Transfer*, vol. 113, pp. 2088–2099, 2012.
6. P. Talukdar, S.C. Mishra, Transient conduction and radiation heat transfer with variable thermal conductivity, *Numerical Heat Transfer, Part A*, vol.41, pp.851–867, 2002.
7. X.L. Xia, Y. Huang, H.P. Tan, X.B. Zhang, Simultaneous radiation and conduction heat transfer in a graded index semitransparent slab with gray boundaries, *Int. J. Heat Mass Transfer*, vol.45, pp. 2673–2688, 2002.
8. S.C. Mishra, N.A. Krishna, N. Gupta, G.R. Chaitanya, Combined conduction and radiation heat transfer with variable thermal conductivity and variable refractive index, *Int. J. Heat Mass Transfer*, vol.51, pp. 83–90, 2008.
9. R. Chaabane, F. askri and S.B. Nasrallah, numerical modeling of boundary conditions for two dimansional conduction heat transfer equation using lattica boltzmann method, *International Journal of Heat and Technology*, vol. 28(2), pp. 51–57, 2010.
10. I. Mejri, A. Mahmoudi, M.A Abbassi , A. Omri, Lattice Boltzmann simulation of conduction-radiation heat transfer in a planar medium, *International Journal of Heat and Technology*, vol. 32, pp. 213–218, 2014.
11. G. Lorenzini, C. Biserni, F.L. Garcia, L.A.O. Rocha, Geometric optimization of a convective T-shaped cavity on the basisof constructal theory, *Int J of Heat and Mass Transfer*, vol. 55, 6951–6958, 2012.
12. G. Lorenzini, L. A. O. Rocha, C. Biserni, E. D. dos Santos, L.A. Isoldi, Constructal Design of Cavities Inserted Into a Cylindrical Solid Body, *ASME Journal of Heat Transfer*, Vol. 134 (7), pp. 0713011 - 0713016, 2012.
13. A. Mahmoudi, I. Mejri, M.A. Abbassi, A. Omri, Analysis of MHD natural convection in a nanofluid-filled open cavity with non uniform boundary condition in the presence of uniform heat generation/absorption, *Powder Technology*, vol.269, 275–289, 2015.
14. A. Mahmoudi, I. Mejri, M.A. Abbassi, A. Omri, Lattice Boltzmann simulation of magnetic field direction effect on natural convection of nanofluid-filled cavity. *International Journal of Heat and Technology*, vol. 32, pp. 9–4, 2014.
15. I. Mejri, A. Mahmoudi, M.A Abbassi , A. Omri, magnetic field effect on natural convection in a nanofluidfilled enclosure with non-uniform heating on both side walls, *International Journal of Heat and Technology*, vol. 32, pp. 127–133, 2014.

NOMENCLATURE

a	Anisotropy factor
c	Speed of light (m/s)
c_p	Specific heat at constant pressure ($JKg^{-1}K^{-1}$)
e_i	Lattice speed (m/s)
f	Internal energy distribution functions (K)
f^{eq}	Equilibrium internal energy distribution (K)
G	Incident radiation (W/m^2)
I	Intensity of radiation (W/m^2)
I^{eq}	Equilibrium intensity (W/m^2)
k	Thermal conductivity ($Wm^{-1}K^{-1}$)
L	Length of the planar geometry (m)
M	Total number of discrete directions
N	Conduction-radiation parameter(=$k\beta/4\sigma T_w^3$)
N_x	Total number of node
p	Scattering phase function
q_R	Heat flux (W/m^2)
S	Source term (W/m^2)
t	Time (s)
T	Temperature (K)
w	Weight in the LBM

GREEK SYMBOLS

Δx Lattice spacing (m)
Δt Time increment (s)
α Thermal diffusivity (m^2/s)
β Extinction coefficient (1/m)
δ Thermal conductivity parameter
ε Emissivity
γ Polar angle (rad)
σ Stefan–Boltzmann constant,5.67 10^{-8} ($W/m^2\ K^4$)
ρ Density (Kg/m^3)
ξ Non dimensional time $(=\alpha\beta^2 t)$
τ Relaxation time for temperature (s)
τ_R Relaxation time for radiation (s)
ω Scattering albedo

SUBSCRIPT

E East
w West